

Drude Metallic Response of Polypyrrole

R. S. Kohlman,¹ J. Joo,¹ Y. Z. Wang,¹ J. P. Pouget,² H. Kaneko,³ T. Ishiguro,³ and A. J. Epstein⁴

¹*Department of Physics, The Ohio State University, Columbus, Ohio 43210-1106*

²*Laboratoire de Physique des Solides (CNRS - URA 2), Université de Paris Sud, 91405 Orsay, France*

³*Department of Physics, Kyoto University, Kyoto 606-01, Japan*

⁴*Department of Physics and Department of Chemistry, The Ohio State University, Columbus, Ohio 43210-1106*

(Received 25 July 1994)

The very highly conducting state of polypyrrole is investigated. A Drude metallic response, similar to the behavior of usual metals, is determined, based on the coincidence of dc and microwave conductivities, measurement of a huge and negative microwave dielectric constant, and the optical determination of an unusual plasma frequency in the far ir. Only a fraction of the conduction electrons participate in the Drude behavior. The real part of the dielectric function shows a second plasma frequency in the near ir, attributed to the remaining conduction electrons, confined due to a lack of homogeneous, three-dimensional order.

PACS numbers: 71.20.Hk, 72.30.+q, 77.84.Jd, 78.66.Qn

The study of metals has been a cornerstone in the understanding of the solid state. Drude established the free electron gas model of metals in 1900, just five years after the experimental discovery of the electron by J. J. Thomson [1]. Despite its simplified assumptions, the Drude model explains high and frequency independent conductivity from the dc to microwave ($\sim 10^{10}$ Hz) frequency range, and a real part of the dielectric constant (ϵ_1) which is negative below the screened plasma frequency where ϵ_1 is zero ($\omega_p^2 \equiv 4\pi n e^2 / m^* \epsilon_b$; n is the density of carriers, e is the electronic charge, m^* is the carrier effective mass, and ϵ_b is the background dielectric constant) [2]. A particular aspect that differentiates metals from nonmetals is that ϵ_1 is huge and negative ($\approx -10^5$) at low frequency ($\omega\tau \ll 1$, where ω is the external frequency and τ is the scattering time). By including interband effects, the full frequency dependence of ϵ of metals can be understood [3].

Many efforts were made to achieve the Drude metallic state in conducting polymers after their discovery in 1977 [4]. However, these initially studied materials were not Drude metals, becoming insulators at low temperature. Recent improvements in chemical processing have produced doped polyacetylene $[(CH)_x]$ [5], polyaniline (PAN) [6,7], and polypyrrole (PPy) [5] with increased conductivity (σ). In some cases, σ remains finite and higher than the minimum metallic conductivity down through the mK range [5]. In others, the polymer still becomes insulating at low temperature [6,7]. A systematic transport and broad frequency optical study on the same samples is necessary to determine the appropriate description of the high and low conductivity states.

In this Letter, we report, to our knowledge, the first measurement of the complete Drude response of a conducting polymer, from dc, through the microwave frequency range, to the plasma frequency in the far ir. For hexafluorophosphate doped PPy [PPy(PF₆)], $\sigma_{dc}(T)$ is nearly identical with the microwave conductivity (σ_{mw}) in T dependence as well as absolute value as expected for the

Drude model. The microwave dielectric constant (ϵ_{mw}) is huge and negative ($\epsilon_{mw} \sim -10^5$ at 265 K). Using the Drude model in the low frequency limit and σ_{mw} and ϵ_{mw} , the Drude plasma frequency (ω_p) is calculated to be in the far ir at ~ 100 cm⁻¹. Optical measurements directly establish a zero crossing of the ϵ_1 in the far ir. This is an independent experimental confirmation of our Drude model prediction based on ϵ_{mw} and σ_{mw} . This plasma frequency is attributed to the most delocalized electrons. An anomalously long scattering time (τ) is estimated as $\sim 3 \times 10^{-11}$ sec, implying an open Fermi surface as expected for highly anisotropic materials [7,8]. A higher plasma frequency ($\equiv \omega_{p1}$) originates predominantly from localized electrons. In contrast to the metallic behavior of PPy(PF₆), ϵ_1 of *p*-toluenesulfonate-doped polypyrrole [PPy(TsO)] is positive in the microwave and optical frequency range, demonstrating that in PPy(TsO), the carriers are localized, consistent with the greater structural disorder. Magnetic susceptibility measurements show a larger density of states at the Fermi level $N(E_F)$ for PPy(PF₆). Taken with the structural studies on the *same* samples, this demonstrates the central effects of structural order. Together, these results point to future use of very highly conducting polymer systems for model studies of insulator-metal transitions, reduced dimensionality effects, and localization.

The detailed method for sample preparation [9] and experimental techniques for σ_{dc} , σ_{mw} , ϵ_{mw} [10], and x-ray diffraction [7] have been reported previously. The optical data were obtained from a Kramers-Kronig analysis of reflectance data, measured with Bomem DA-2 FTIR ($50-10^4$ cm⁻¹) and Perkin-Elmer Lambda-19 UV-VIS ($5 \times 10^3-5 \times 10^4$ cm⁻¹) spectrometers, the latter equipped with an integrating sphere [11]. The optical data were extrapolated to $\omega = 0$ using the Hagen-Rubens approximation scheme and at high frequency ($5 \times 10^4-10^5$ cm⁻¹) with a reflectance $R \propto \omega^{-2}$ (interband) followed by an $R \propto \omega^{-4}$ (free electron) extrapolation

for higher frequencies ($\geq 10^5 \text{ cm}^{-1}$) [12]. The magnetic susceptibility was measured using a Bruker ESP-300 EPR spectrometer [10].

Figure 1(a) compares $\sigma_{dc}(T)$ with $\sigma_{mw}(T)$ for PPy(PF₆). The absolute values and the temperature dependence in the dc and microwave frequency ranges are nearly identical, in agreement with the Drude theory. However, unlike usual metals, σ very slowly decreases as temperature decreases from RT ($\sigma_{dc} \sim 300 \text{ S/cm}$) to $\sim 20 \text{ K}$, and $d\sigma/dT < 0$ for $T < 20 \text{ K}$. The ratio of $\sigma(RT)/\sigma(20 \text{ K})$ is < 1.8 , relatively small in comparison

to that of other highly conducting polymers (e.g., see Refs. [6,7]). We plot the reduced activation energy [13] ($W \equiv d \ln \sigma / d \ln T$) vs T [inset Fig. 1(a)]. The decrease of W with decreasing T implies that the system is in the metallic regime.

Figure 1(b) shows $\epsilon_{mw}(T)$ for PPy(PF₆) materials. The ϵ_{mw} at 265 K is huge and negative, $\sim -10^5$, corresponding to the Drude dielectric response at microwave frequencies. The ϵ_{mw} remains huge and negative down to 4.2 K ($\sim -4 \times 10^4$). There is a very weak T dependence of ϵ_{mw} and a maximum of ϵ_{mw} at $\sim 20 \text{ K}$. This behavior qualitatively agrees with $\sigma_{dc}(T)$ and $\sigma_{mw}(T)$. The $\epsilon_{mw}(T)$ reported for other polymer metals [(CH)_x or PAN] has a stronger T dependence [7,14]. In the Drude model in the low frequency limit ($\omega\tau \ll 1$), $\sigma_{mw} \approx (\omega_p^2/4\pi)\tau$ and $\epsilon_{mw} \approx -\omega_p^2\tau^2$. Hence, ω_p and τ ($\approx 4\pi\epsilon_{mw}/\sigma_{mw}$) are $\sim 0.01 \text{ eV}$ ($\sim 100 \text{ cm}^{-1}$) and $\sim 3 \times 10^{-11} \text{ sec}$, respectively. This very small ω_p in the far ir likely originates from the most delocalized electrons of the conduction band. The measured τ is anomalously long compared to that of alkali or transition metals ($10^{-13} \sim 10^{-14} \text{ sec}$), which indicates that the sample has an open Fermi surface as expected for highly anisotropic materials.

Optical studies on parts of the *same* sample enable a direct measurement in the frequency range of the predicted far ir plasma frequency. The reflectance of PPy(PF₆) shows two distinct frequency regimes [Fig. 2(a)]. In the far ir ($\leq 300 \text{ cm}^{-1}$), the reflectance increases steeply toward unity, approaching 95% at 50 cm^{-1} . Above 2000 cm^{-1} , the frequency dependence is weaker up to the plasma frequency at $\sim 17000 \text{ cm}^{-1}$. The oscillations in the mid ir ($500\text{--}2000 \text{ cm}^{-1}$) are due to phonons.

The real part of the dielectric function (ϵ_1) [Fig. 2(b)] reveals a variety of excitations. In the far ir, ϵ_1 of PPy(PF₆) is negative, crossing from negative to positive at $\omega_p \sim 250 \text{ cm}^{-1}$, the screened plasma frequency. The presence of ω_p in the far ir with $\epsilon_1 < 0$ for the lowest measured optical frequencies confirms the microwave range prediction of a free carrier plasma resonance in the far ir. Between $\omega_p = 250$ and 500 cm^{-1} , ϵ_1 is positive. At 500 cm^{-1} , ϵ_1 turns negative again but with increasing frequency turns positive once more at a second screened plasma frequency $\omega_{p1} \approx 8800 \text{ cm}^{-1}$. The presence of ω_{p1} in the near ir, which shows Lorentzian frequency dispersion, indicates that most of the conduction electrons are bound (localized) [12].

It is of interest to compare the behavior of metallic PPy(PF₆) with slightly less conducting [$\sigma_{dc}(295 \text{ K}) \approx 100 \text{ S/cm}$] PPy(TsO) with the same doping level. The degree of crystallinity of PPy(TsO) is $\sim 25\%$, approximately one-half that of PPy(PF₆), with a crystalline domain size which is decreased to $\sim 15 \text{ \AA}$ compared to $\sim 20 \text{ \AA}$ [15]. The bulky TsO dopant not only increases the separation between (b,c) layers of PPy chains by 50% but likely enhances the conformational disorder of the PPy chain since intrachain x-ray reflections are not recorded for PPy(TsO).

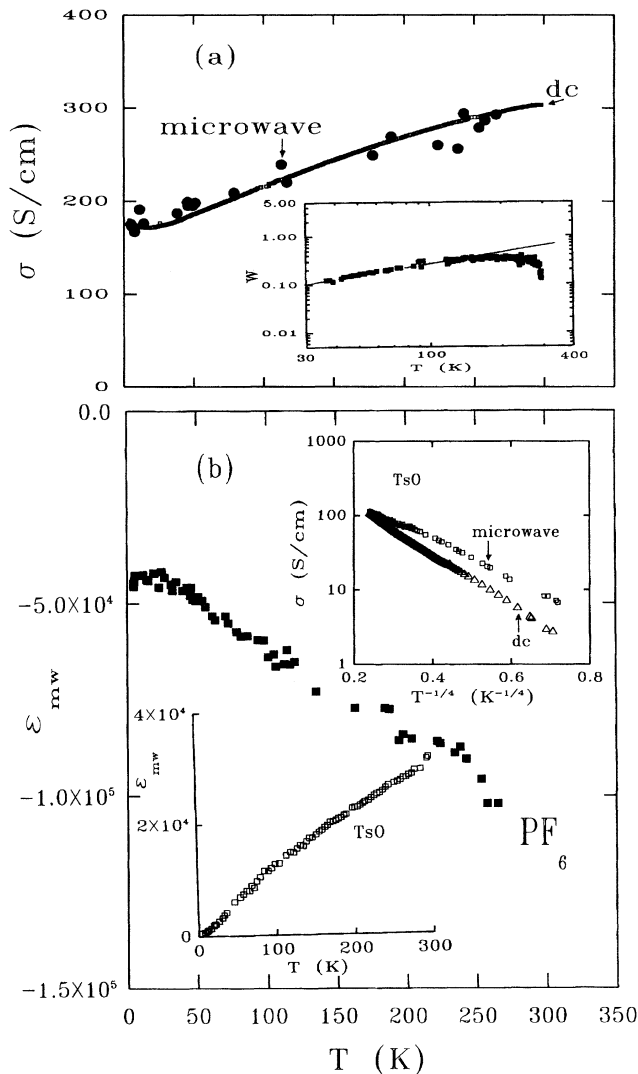


FIG. 1. (a) Comparison of dc (small square) and microwave (solid circle) conductivities of PPy(PF₆) as a function of temperature. Inset: the reduced activation energy (W) vs T for PPy(PF₆). (b) $\epsilon_{mw}(T)$ for PPy(PF₆). Top inset: comparison of dc (small triangle) and microwave (open square) σ of PPy(TsO). Bottom inset: $\epsilon_{mw}(T)$ for PPy(TsO).

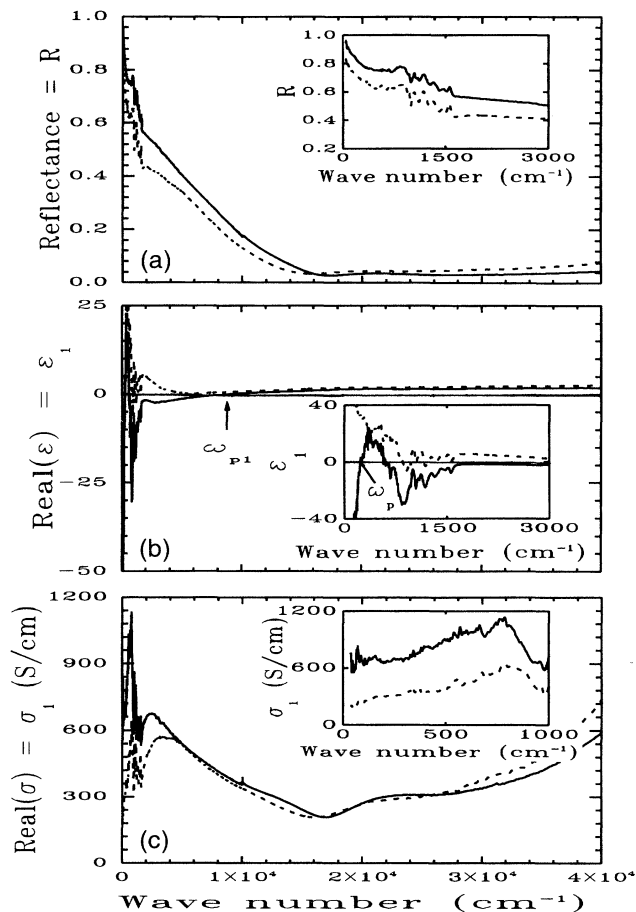


FIG. 2. Comparison of the optical data of PPy(PF₆) (solid lines) and PPy(TsO) (broken lines) at room temperature as a function of frequency. (a) Reflectance data. Inset: magnification of reflectance below 3000 cm⁻¹. (b) Real part of the dielectric constant. Inset: magnification of ϵ below 3000 cm⁻¹. (c) Optical conductivity. Inset: magnification of optical conductivity below 1000 cm⁻¹.

The optical conductivity (σ_1) is higher for PPy(PF₆) than PPy(TsO) up to ~ 17000 cm⁻¹ [Fig. 2(c)]. σ_1 for PPy(PF₆) is constant from the lowest measured frequency, 50 cm⁻¹, to $\omega_p = 250$ cm⁻¹ as expected for a Drude metal. Above ω_p , σ_1 increases due to the contributions of localized electrons. It reaches a maximum (ignoring phonon features) of 680 S/cm at ~ 2500 cm⁻¹ and then begins to decrease with increasing frequency. σ_1 of more disordered PPy(TsO) does not reach its maximum of 550 S/cm until approximately 4000 cm⁻¹ and decreases more rapidly (non-Drude-like) for $\omega < \omega_p$. Above 17000 cm⁻¹, interband transitions dominate σ_1 [16].

In contrast to PPy(PF₆), $\epsilon(\omega)$ of PPy(TsO) remains positive, increasing rapidly with decreasing frequency in the far infrared [Fig. 2(b)]. This response is characteristic of a large density (n) of confined carriers [12]. Thus, the optical data show no evidence for free carriers in more disordered PPy(TsO).

The insets of Fig. 1(b) show the temperature-dependent conductivity and dielectric constant of PPy(TsO) materials. Though its room temperature σ_{dc} is one-third that of PPy(PF₆), its ϵ_{mw} is positive in the entire temperature range indicating localization behavior as shown in the lower inset of Fig. 1(b). The $T \rightarrow 0$ localization length is estimated as ~ 25 Å using the metallic box model [10] and the ESR $N(E_F)$ (see below), in agreement with the crystalline coherence length ($\xi \sim 15$ Å). ϵ_{mw} linearly increases as temperature increases even though the localization length is small, which implies that the charge can easily delocalize through the disordered regions, and the phase segregation between the metallic and disordered regions is weak in the PPy(TsO) system. The upper inset of Fig. 1(b) compares the temperature-dependent dc and microwave conductivities based on a 3D variable-range-hopping (VRH) model; $\sigma_{dc}(T) = \sigma_0 \exp[-(T_0/T)^{1/4}]$, where $T_0 = 16/k_B N(E_F) L^3$ (k_B : Boltzmann constant). Using the slope $T_0 \approx 4100$ K and $N(E_F) = 0.2$ states/eV ring (see below), $L \sim 30$ Å. This independent estimate of localization length is also comparable with the x-ray crystalline coherence length (ξ). The stronger temperature dependence of σ_{dc} in comparison with $\sigma_{mw}(T)$ implies that the sample is in the localized regime [17].

The spin susceptibility, Fig. 3, provides additional insight into the metallic state and the effects of disorder. The solid lines are fits to $\chi T = \chi_P T + C$ where χ_P is the temperature independent Pauli susceptibility and C is the Curie constant. The positive slope in Fig. 3 indicates a finite $N(E_F)$ for both materials: PPy(PF₆), $N(E_F) \approx 0.80$ states/eV ring; and PPy(TsO), $N(E_F) \approx 0.20$ states/eV ring. PPy(TsO) shows a larger Curie component (uncorrelated spins). The smaller $N(E_F)$ of PPy(TsO) is in agreement with a smaller fraction of the sample having three-dimensional order [15] and the metallic Pauli susceptibility being associated with the three dimensionally ordered regions, similar to doped polyanilines [18].

The agreement of the dc and microwave conductivities, the negative microwave dielectric constant, and the observation of the far ir plasma frequency (ω_p) iden-

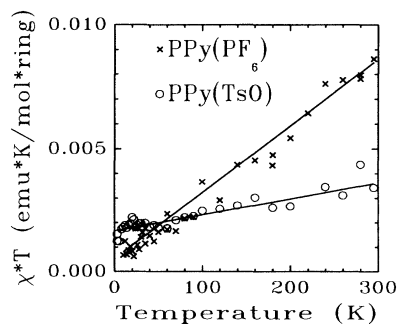


FIG. 3. χT vs T for PPy(PF₆) (crosses) and PPy(TsO) (circles).

tify the presence of free, Drude carriers in PPy(PF₆). Comparing the far ir Drude plasma frequency with the plasma frequency expected for the full carrier density n_0 (one conduction electron per three ring repeat, as determined by elemental analysis [9]) with $m^* = m_e$, we find $n/m^* \approx 10^{-4}n_0/m_e$. This small value of n/m^* suggests that only a very small fraction of the total number of conduction electrons are delocalized sufficiently to participate in the free electron Drude response. We suggest that these electrons are able to diffuse between three dimensionally ordered regions (crystalline domains) without being localized. It is noted that the m^* for these electrons may be large as these electrons must traverse the disordered regions, within which the conduction electron bandwidth is narrowed. Weak localization and phonon induced delocalization in one-dimensional links through the disordered regions likely determine the T dependence of the dc and microwave conductivity [19]. These most delocalized electrons have an anomalously long scattering time (τ) which is attributed to the ramifications of an open Fermi surface. The large majority of conduction electrons are confined, resulting in the larger ω_{p1} . Fittings of the reflectance data [20] indicate that the carriers which contribute to ω_{p1} are bound by an energy of order 0.2 eV in PPy(PF₆) and 0.3 eV in PPy(TsO).

In summary, Drude type metallic behavior has been demonstrated for the first time in a polymer metal. This conclusion is based on measurements in the same samples of coincidence of σ_{dc} and σ_{mw} , huge and negative microwave ϵ_1 , and direct spectroscopic observation of ω_p consistent with the microwave frequency Drude analysis. The measured long τ_{mw} supports an open Fermi surface. The measured two plasma frequencies (ω_p and ω_{p1}) reflect the inhomogeneity of local order: The ω_p is due to the most delocalized electrons, and ω_{p1} originates from confined electrons. The increase of crystalline order correlates with the improved conductivity and the increase in $N(E_F)$ in PPy(PF₆) over PPy(TsO) as well as the presence of Drude free carriers. In contrast to the metallic behavior of PPy(PF₆), PPy(TsO) is nonmetallic with localized behavior through the dc, microwave, and optical frequency range.

We thank V.N. Prigodin for useful discussions and T. Lemberger for experimental assistance. This work was partially supported by the International Joint Research Project from NEDO (The New Energy and Industrial Technology Development Organization), and ONR.

- [1] P. Drude, *Ann. Phys.* **1**, 566 (1900); **3**, 369 (1900).
- [2] G. Burns, *Solid State Physics* (Academic, New York, 1985).
- [3] H. Ehrenreich and H.R. Phillip, *Phys. Rev.* **128**, 1622 (1962).
- [4] C.K. Chiang, C.R. Fincher, Jr., Y.W. Park, A.J. Heeger, H. Shirakawa, E.J. Louis, S.C. Gau, and A.G. MacDiarmid, *Phys. Rev. Lett.* **39**, 1098 (1977).
- [5] T. Ishiguro, H. Kaneko, Y. Nogami, H. Ishimoto, H. Nishiyama, J. Tsukamoto, A. Takahashi, M. Yamaura, T. Hagiwara, and K. Sato, *Phys. Rev. Lett.* **69**, 660 (1992).
- [6] M. Reghu, Y.O. Yoon, D. Moses, A.J. Heeger, and Y. Cao, *Phys. Rev. B* **48**, 17685 (1993); M. Reghu, Y. Cao, D. Moses, and A.J. Heeger, *ibid.* **47**, 1758 (1993).
- [7] J. Joo, Z. Oblakowski, G. Du, J.P. Pouget, E.J. Oh, J.M. Wiesinger, G. Min, A.G. MacDiarmid, and A.J. Epstein, *Phys. Rev. B* **49**, 2977 (1994), and references therein.
- [8] S. Kivelson and A.J. Heeger, *Synth. Met.* **22**, 371 (1988).
- [9] K. Sato, M. Yamaura, T. Hagiwara, K. Murata, and M. Tokumoto, *Synth. Met.* **40**, 35 (1991); M. Yamaur, T. Hagiwara, and K. Iwata, *ibid.* **26**, 209 (1988).
- [10] Z.H. Wang, E.M. Scherr, A.G. MacDiarmid, and A.J. Epstein, *Phys. Rev. B* **45**, 4190 (1992).
- [11] R.P. McCall, E.M. Scherr, A.G. MacDiarmid, and A.J. Epstein, *Phys. Rev. B* **50**, 5094 (1994).
- [12] F. Wooten, *Optical Properties of Solids* (Academic, New York, 1972).
- [13] A.G. Zabrodski and K.N. Zeninova, *Zh. Eksp. Teor. Fiz.* **86**, 727 (1984) [*Sov. Phys. JETP* **59**, 425 (1984)].
- [14] J. Joo, G. Du, V.N. Prigodin, J. Tsukamoto, and A.J. Epstein (to be published).
- [15] Y. Nogami, J.P. Pouget, and T. Ishiguro, *Synth. Met.* **62**, 257 (1994); J.P. Pouget, Z. Oblakowski, Y. Nogami, P.A. Albouy, M. Laradjani, E.J. Oh, Y. Min, A.G. MacDiarmid, J. Tsukamoto, T. Ishiguro, and A.J. Epstein, *Synth. Met.* **65**, 131 (1994). The crystalline coherence lengths, percent crystallinity, and $\sigma_{dc}(T)/\sigma_{dc}(300\text{ K})$ of both stretched and unstretched materials of PPy(PF₆) are similar, though the absolute values of conductivity differ.
- [16] K. Yakushi, L.J. Lauchlan, T.C. Clarke, and G.B. Street, *J. Chem. Phys.* **79**, 4774 (1983).
- [17] A.R. Long, *Adv. Phys.* **31**, 553 (1982); E.P. Nakhmedov, V.N. Prigodin, and A.V. Samukhin, *Sov. Phys. Solid State* **31**, 368 (1989).
- [18] J.M. Ginder, A.F. Richter, A.G. MacDiarmid, and A.J. Epstein, *Solid State Commun.* **63**, 97 (1987).
- [19] V.N. Prigodin and K.B. Efetov, *Phys. Rev. Lett.* **70**, 2932 (1993).
- [20] R. Kohlman *et al.* (to be published).